

SIMULTANEOUS IDENTIFICATION OF AERODYNAMIC STATES FOR A TRANSONIC TYPICAL SECTION

João Henrique A. Azevedo, joaohenrique.azevedo@gmail.com

Instituto Tecnológico de Aeronáutica, 12228-900 São José dos Campos, SP, Brazil

João Luiz F. Azevedo, joaoluiz.azevedo@gmail.com

Roberto Gil A. Silva, roberto.gil.silva@gmail.com

Instituto de Aeronáutica e Espaço, 12228-903 São José dos Campos, SP, Brazil

Abstract. *The objective of the present work is to study forms of identifying the aerodynamic states, for state space aeroelastic stability analyses in the frequency domain, using high-fidelity CFD codes in an efficient fashion. In particular, there is interest in the use of non-parametric identification techniques in order to obtain the necessary aerodynamic transfer functions from a single unsteady CFD computation. The work implements a single combined input method in order to simultaneously excite the aerodynamic responses in all the system natural modes and, at the same time, allow the output to be split into the contribution of each individual mode to the aerodynamic transfer function. The proposed approach is applied to a NACA 0012 airfoil-based typical section model in transonic flight.*

Keywords: *System identification, Aerodynamic states, Flutter prediction*

1. INTRODUCTION

It is well-known that, in recent years, computational fluid dynamics (CFD) techniques have played an increasingly important role in many applications which require understanding the aerodynamics of a given configuration. This statement also holds for aeroelastic analyses. However, the use of high-fidelity CFD solvers, based on the Euler or the Navier-Stokes equations, usually leads to fairly long computational times, especially for the unsteady calculations that would be required in aeroelasticity. Hence, the actual issue addressed in the present work is the matter of reducing the computational cost of such CFD calculations such that the overall cost of an aeroelastic study would be acceptable in industrial conditions. The present effort builds upon previous work by [Marques and Azevedo \(2008a,b\)](#), which used unsteady CFD solutions to impulsive and indicial perturbations in each structural mode of the configuration in order to build the required aerodynamic transfer functions and, then, identify aerodynamic states that would allow aeroelastic stability analyses in the frequency domain. The drawback with such approach is that the construction of an aeroelastic stability root locus, for a given flight condition, costs one steady CFD run, in order to obtain the initial steady state solution at the flight condition of interest, plus as many unsteady CFD runs as the number of mode shapes considered in the analysis. For a real engineering problem, in which typically some 30 or more modes are considered, this cost is not yet acceptable.

Therefore, the objective of the present work is to use of non-parametric system identification techniques in order to obtain the necessary aerodynamic transfer functions from a single unsteady CFD computation. The approach adopted here follows the work of [Raveh \(2001, 2004\)](#), [Kim et al. \(2005\)](#) and [Silva \(2008\)](#). The paper discusses the details of the methodology adopted in as much detail as the available space allows, and it applies the proposed approach to a NACA 0012 airfoil-based typical section model in transonic flight.

The CFD tool used here is based on the 2-D Euler equations. These equations are discretized using a finite volume approach for unstructured grids. A centered scheme, with added artificial dissipation, is used for spatial discretization and explicit Runge-Kutta methods are employed for time marching. Afterwards, the work implements a single combined input method in order to simultaneously excite the aerodynamic responses in all the natural modes of the configuration and, at the same time, allow the output to be split into the contribution of each individual mode to the aerodynamic transfer function. The technique for identifying these transfer functions is based on the calculation of the power spectral densities

of the inputs and outputs of the system.

2. FLOW SOLVER AND MESH MOVEMENT

The CFD tool applied in this work is based on the 2-D Euler equations, which represent two-dimensional, compressible, rotational, inviscid and nonlinear flows. Due to the use of unstructured meshes and the adoption of the finite volume approach, these equations are written in Cartesian form. Furthermore, as usual in CFD applications, flux vectors are employed and the equations are nondimensionalized. Hence, they can be written as

$$\frac{\partial}{\partial t} \iint_{\Omega} Q dx dy + \int_S (E dy - F dx) = 0. \quad (1)$$

In Eq. 1, Ω represents the volume of the control volume or, more precisely, its area in the two-dimensional case. S is its surface, or its side edges in 2-D. Q is the vector of conserved properties of the flow, given by

$$Q = \left[\rho \quad \rho u \quad \rho v \quad e \right]^T. \quad (2)$$

E and F are the inviscid flux vectors in the x and y directions, respectively, defined as

$$E = \left\{ \begin{array}{c} \rho U \\ \rho u U + p \\ \rho v U \\ (e + p)U + x_t p \end{array} \right\}, \quad F = \left\{ \begin{array}{c} \rho V \\ \rho u V \\ \rho v V + p \\ (e + p)V + y_t p \end{array} \right\}. \quad (3)$$

The nomenclature adopted here is the usual one in CFD: ρ is the density, u and v are the Cartesian velocity components and e is the total energy per unity of volume. The pressure, p , is given by the perfect gas equation, written as

$$p = (\gamma - 1) \left[e - \frac{1}{2} \rho (u^2 + v^2) \right]. \quad (4)$$

Once again, as usual, γ represents the ratio of specific heats. The contravariant velocity components, U and V , are determined by

$$U = u - x_t \quad \text{and} \quad V = v - y_t, \quad (5)$$

where x_t and y_t are the Cartesian components of the mesh velocity in the unsteady case.

The aerodynamic equations are discretized using a cell centered, finite volume scheme. Spatial discretization is equivalent to a centered scheme (Jameson and Mavriplis, 1986; Mavriplis, 1990). As usual with centered schemes, artificial dissipation terms must be added to the discretized equations in order to maintain numerical stability, especially near shock waves. In the present case, the artificial dissipation operator is constructed as a blend of second and fourth difference terms (Jameson *et al.*, 1981) with coefficients that are proportional to local pressure gradients.

After the complete spatial discretization and the inclusion of the artificial dissipation terms, the Euler equations can be written for the i -th volume as

$$\frac{d}{dt} (\Omega_i Q_i) + C_i - D_i = 0, \quad (6)$$

where C and D represent the convective and the artificial dissipation operators, respectively. Equation 6 is advanced in time using a second-order accurate, 5-stage, explicit, hybrid Runge-Kutta time stepping scheme (Jameson and Mavriplis, 1986; Mavriplis, 1990). The convective operator is evaluated at every stage of the integration process, but the artificial dissipation operator is only evaluated at the two initial stages (Jameson *et al.*, 1981). Moreover, convergence acceleration

techniques, such as local time stepping and implicit residual smoothing (Jameson *et al.*, 1981; Jameson and Baker, 1987), are employed in steady calculations in order to guarantee an acceptable computational efficiency in steady-state mode. Further details on the approach here used for the numerical discretization of the Euler equations and on the construction of the present code can be seen in Marques and Azevedo (2008a).

The meshes used in the present work are generated with the commercial grid generator ICEM CFD[®]. Since unsteady calculations involve body motion, the computational mesh should be somehow adjusted to take this motion into account. One way of accounting for the motion of the body is to rigidly move the mesh together with the airfoil. In the present work, since a standard typical section model is of interest, only rigid body mode are involved. Therefore, it is simpler and less expensive to move the mesh rigidly with the airfoil then, for instance, deforming the mesh to accommodate for the airfoil movement (Marques and Azevedo, 2008a).

3. STATE SPACE FORMULATION AND SYSTEM IDENTIFICATION

If one is interested in representing the aerodynamic forces in the frequency domain, the system can be conveniently studied in the Laplace domain. As such, a state space representation of the typical section system can be written as (Marques and Azevedo, 2008b)

$$\bar{s} \left[\tilde{M} \right] \{X(\bar{s})\} + \left[\tilde{K} \right] \{X(\bar{s})\} = \left\{ \tilde{Q}(\bar{s}) \right\}, \quad \text{where} \quad \bar{s} = \frac{s}{\omega_r} \quad (7)$$

is the dimensionless Laplace transform complex variable and ω_r is a reference circular frequency. The idea behind this procedure is to evaluate the aerodynamic influence coefficient matrix over a reduced frequency range of interest and, by making use of the analytical continuation principle (Churchill, 1974), to extend such result to the entire complex plane.

The data, that would come from the CFD solver, however, even after an appropriate identification of the aerodynamic transfer functions in the frequency domain, would consist of sets of numerical values of the aerodynamic coefficients as a function of (reduced) frequency. This format of the aerodynamic data is not convenient for the solution of Eq. 7. One approach for dealing with the problem consists in approximating these data using interpolating polynomials, which then would lead to the creation of (new) aerodynamic states. The literature reports on a number of different interpolating polynomials that could be used in the present case, and the interested reader is referred to Marques and Azevedo (2008b) for a detailed discussion of this issue. In any event, regardless of which specific polynomial is used for the representation of the aerodynamic response in the Laplace domain, the resulting state space representation of the typical section aeroelastic system can be written as

$$\{\dot{\chi}(\bar{t})\} = [D] \{\chi(\bar{t})\}. \quad (8)$$

Here, $\{\chi(\bar{t})\}$ is the new state vector that results from the addition of the aerodynamic state variables, and $[D]$ is the system dynamic matrix. This matrix is defined in terms of the system mass and stiffness matrices, and of other matrices which appear from the interpolating polynomial representation of the aerodynamic forces. Further details can, again, be seen in Marques and Azevedo (2008b). Finally, the aeroelastic stability analysis of the system can, then, be reduced to the classical eigenvalue problem, for each value of some characteristic parameter. Typically, the characteristic parameter is a reduced speed (U^*) or a reduced dynamic pressure.

The main assumption being adopted here is that the system can be considered linear. However, the use of a high-fidelity CFD solver is justified for the transonic flight regime due to its inherent nonlinear behavior. On the other hand, as shown in Marques and Azevedo (2008a), there is an amplitude range in which the aerodynamic response due to the unsteady motion can be considered linear with respect to the mode shapes, even in the transonic regime. Therefore, assuming that the motion amplitude is sufficiently small, one can formulate the problem as a linear dynamic system in the frequency domain.

The traditional approach to identifying the system's dynamic matrix is to provide an excitation signal in one of the

inputs and measure the outputs. This requires, however, a number of unsteady simulations equal to the number of modes considered in the system. If, on the other hand, one multiplies the convolution sum equation for a given output by one of the inputs, considers the expected value and uses the Wiener-Khintchin relations (Isermann and Münchhof, 2011), one can rewrite the input-output relation as

$$P_{y_k u_i} = \sum_{j=1}^n (G_{kj} P_{u_j u_i}) , \quad (9)$$

where $P_{y_k u_i}$ is the cross power spectral density of the output y_k and the input u_i and $P_{u_j u_i}$ is the cross power spectral density of the inputs u_j and u_i . Assuming that uncorrelated input signals are employed, the cross cross power spectral density of two different inputs is zero. If such, the system can be excited simultaneously in all of the modes considered in the problem and the transfer functions can be estimated by a division, in the frequency domain, between the output-input cross power spectral densities and the input power spectral density.

One possible set of uncorrelated input signals can be obtained with the use of Walsh functions (Silva, 2008). As noted by Silva (2008), this family of functions has a similarity to step inputs and, therefore, embodies the impulsive nature of step inputs with regard to frequency bandwidth. Each one of these functions may be seen as a line, or a column, of a Hadamard (1893) matrix of order 2^n . In order to construct these matrices, the authors have employed the method proposed by Sylvester (1867), in which a Hadamard matrix H_{2^n} is defined recursively by

$$H_{2^n} = \begin{bmatrix} H_{2^{n-1}} & H_{2^{n-1}} \\ H_{2^{n-1}} & -H_{2^{n-1}} \end{bmatrix} , \quad (10)$$

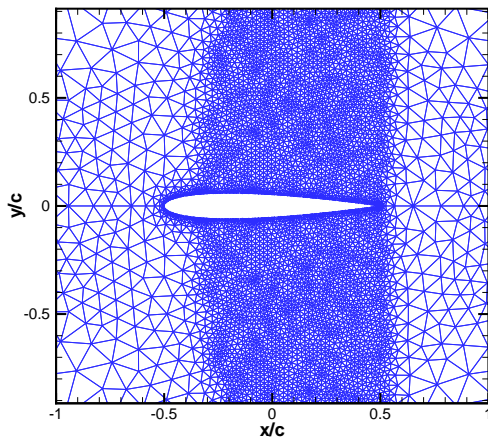
where H_1 is the unitary identity matrix. Each element of a row is, then, assigned as the magnitude of the corresponding step block in a Walsh function.

4. RESULTS

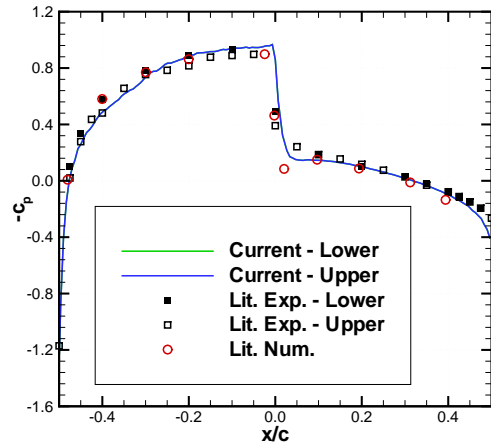
The test case considered throughout this paper involves a NACA 0012 airfoil at $M_\infty = 0.8$ and $\alpha_0 = 0$. In order to perform unsteady calculations, an initial steady-state solution must be obtained prior to initiating the unsteady CFD runs. Such solution is obtained by the same CFD code, running in steady mode, *i.e.*, with a variable time step method, which is converged to machine zero. Since the numerical method implemented in the code provides steady-state solutions which are independent of the time step, such converged solution can, now, be used as the initial condition for all the unsteady calculations in the present work.

Pressure coefficient results for the initial steady-state solution for the present case are shown in Fig. 1. As one can see, the present results are capable of representing the physical phenomena expected for the flows of interest, including the strong shock waves that occur over the airfoil. Figure 1 (a) presents pressure coefficient contours for the flowfield near the airfoil, whereas Fig. 1 (b) shows the pressure coefficient distribution over the airfoil surface. Comparisons with the numerical results available in Kroll and Jain (1987) (Lit. Num.) and experimental ones found in McDevitt and Okuno (1985) (Lit. Exp.) are also shown in Fig. 1 (b). The current results present a small oscillation in the pressure coefficient distribution in the region prior to the shock wave and in the vicinity of the trailing edge. These discrepancies, however, do not affect the overall adequateness of the solution and this is rather confirmed by the good agreement between the current solution and that of Kroll and Jain (1987). Moreover, although one cannot expect Euler results to exactly match experimental measurements, Fig. 1 (b) shows that, except for the aforementioned regions, the numerical pressure coefficient distribution is very close to the experimental one. Therefore, one may consider the current computational results to be in good agreement with the experimental and numerical data in the literature.

From the converged stationary solution, the mesh is rigidly moved in a prescribed pattern and a total of 100,000 time steps of unsteady flow are computed with a constant Δt of 0.003 dimensionless time units. Furthermore, the maximum amplitudes considered here are 0.000001 c for the plunging mode and 0.0001 deg. for the pitching degree of freedom.



(a) Mesh view around the NACA 0012 airfoil.

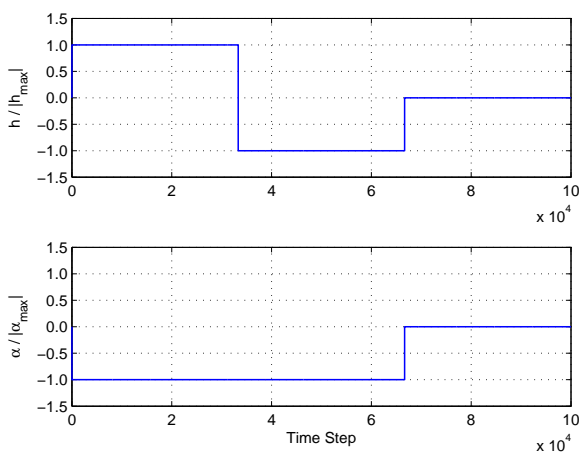


(b) Pressure coefficient distribution over airfoil.

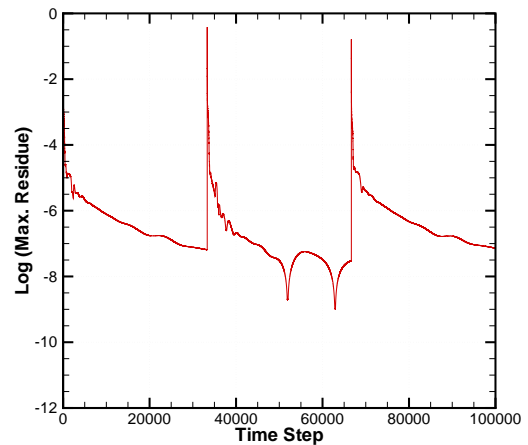
Figure 1. Steady-state solution for a NACA 0012 airfoil at $M_\infty = 0.8$ and $\alpha_0 = 0$.

The reason for choosing such low amplitudes, as discussed earlier, is to remain within the “quasi-linear” region around the nonlinear steady solution and to allow the CFD code to accurately propagate the disturbances from the discrete motion (Raveh, 2001). Further discussion of the effects of the amplitudes of modal motions, in the context of the present CFD solver, are presented in Marques and Azevedo (2008a). Finally, a modified Walsh function set was considered here in order to prescribe the airfoil motion. This modification consists of a blank region at the end of the unsteady run as illustrated in Fig. 2 (a). This zero-motion region attempts to guarantee that the computation starts and ends with a solution without any perturbations from the prescribed motion. The size of this blank region also influences the size of the window function to be considered and, therefore, the resolution in the frequency domain. Many configurations have been studied by the authors with sets of different sizes of zero-motion regions and locations, some of which are presented in Azevedo et al. (2012). The authors have chosen to present the results from the set illustrated in Fig. 2 (a) in the present paper because such results have a better resolution in the frequency domain than those presented in Azevedo et al. (2012).

A better visualization of the perturbations created by the different motions, for the present unsteady simulations, can be inferred from a plot of the residue time histories. It is true that the concept of residue does not really apply to unsteady calculations, but nevertheless it is helpful in the present case. Figure 2 (b) presents the time history of the L_∞ norm of the density residues for the unsteady calculations using the set of Walsh function inputs here considered. When the body is



(a) Normalized motions prescribed by the Walsh function (WF) input.



(b) Maximum density residue throughout the unsteady calculations.

Figure 2. Input and output from the unsteady CFD solver.

moved according to the prescribed pattern shown in Fig. 2 (a), a spike can be seen in the residue curve. As the aerodynamic

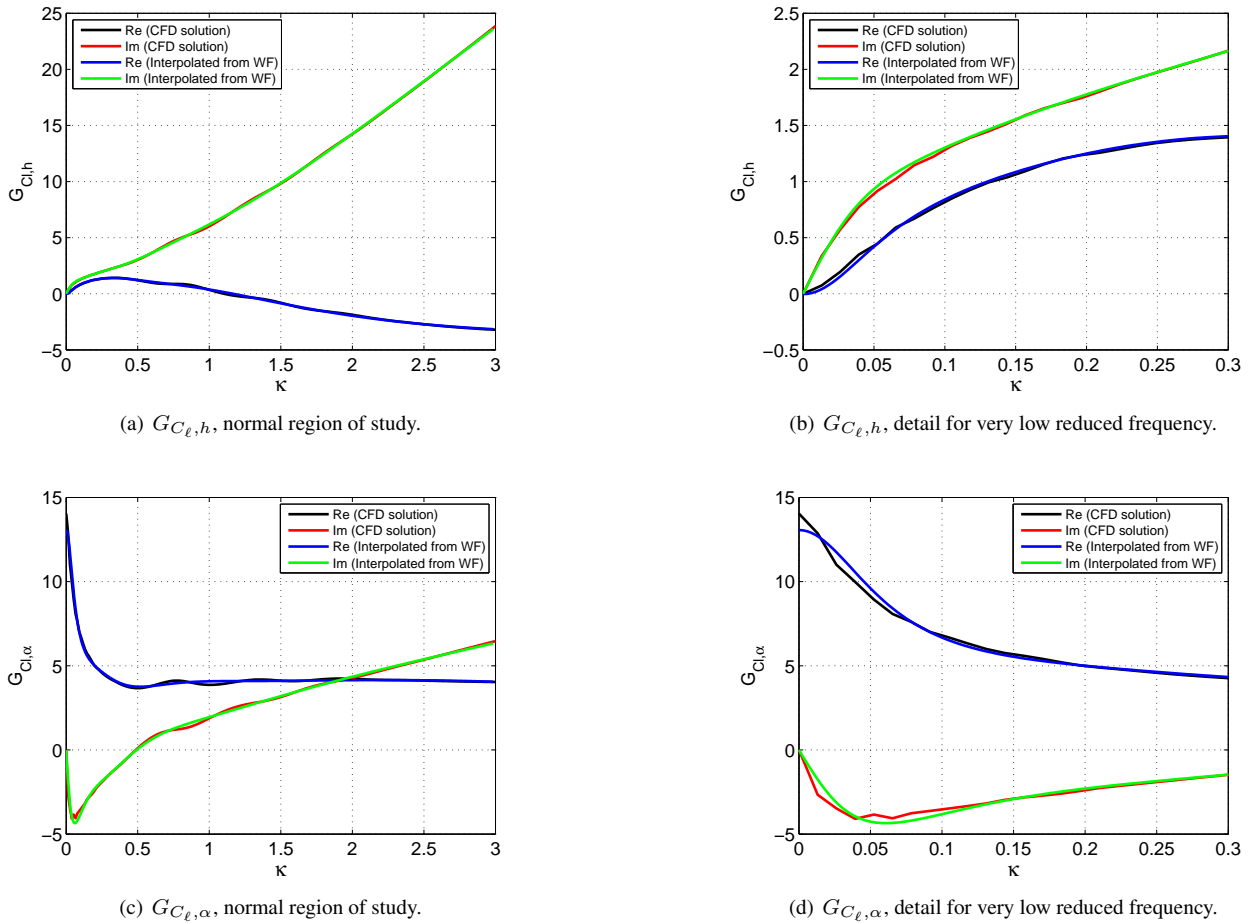
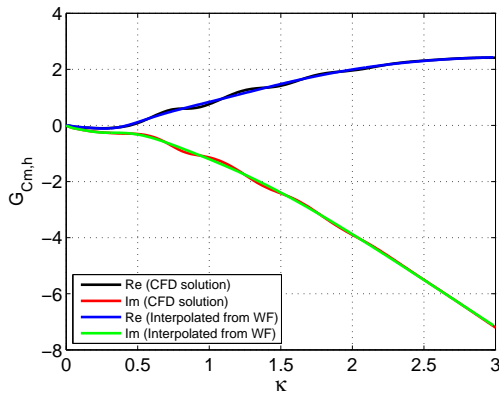


Figure 3. $G_{C_{l,h}}$ and $G_{C_{l,\alpha}}$ transfer functions at low reduced frequencies.

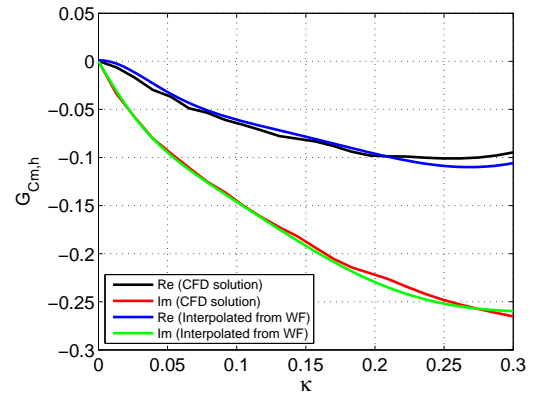
perturbations from the motion die out, there is a marked decrease in the residue of the calculation, as indicated in Fig. 2 (b). This figure also shows that there is a significant decrease of the perturbations prior to the next motion being prescribed in the set of Walsh functions used. The fact that the residues quickly decay after a given perturbation is an indication that the amplitudes of motion here used are adequate and the CFD code is capable of handling the perturbation velocities so generated.

Marques and Azevedo (2008a) present frequency domain responses for the transonic configuration in question when the airfoil is submitted to both plunging and pitching motions. These responses are obtained numerically with a solver very similar to the one used in the present work. The present authors reproduced these solutions using discrete step and the set of Walsh function inputs, here described, in order to validate the present capability of obtaining the aerodynamic transfer functions. The validation results can be seen in Azevedo *et al.* (2012). For the results in the present paper, the WF inputs shown in Fig. 2 (a) are used in order to generate the aerodynamic transfer functions following the methodology previously described.

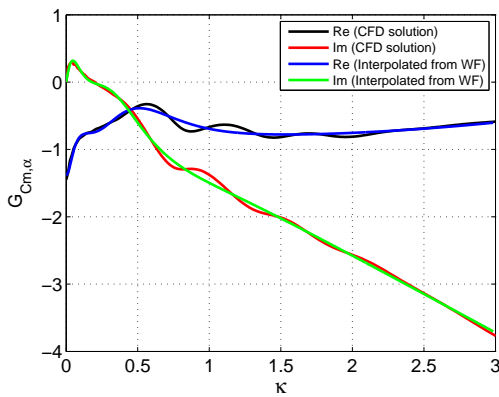
The last stage in preparing the data generated by the CFD calculations in order to be able to perform aeroelastic stability analyses in the frequency domain consists in approximating the string of transfer function values by an interpolating polynomial. In the present work, the interpolating polynomials proposed by Eversman and Tewari (1991) without any provision for the treatment of repeated, or very close, poles are used. All calculations in this paper considered the interpolating polynomials with the addition of 6 poles. Moreover, as described in Marques and Azevedo (2008b), the interpolating polynomials are obtained by a least-squares fitting of the transfer functions generated from the CFD results. Figure 3 presents the comparison for the results for the $C_{l\ell}$ transfer functions. All plots are showing the real and imaginary parts of the approximated transfer functions given by the interpolating polynomials, which are compared to the original transfer functions obtained directly from the CFD solution using the WF inputs. It should be observed that these approx-



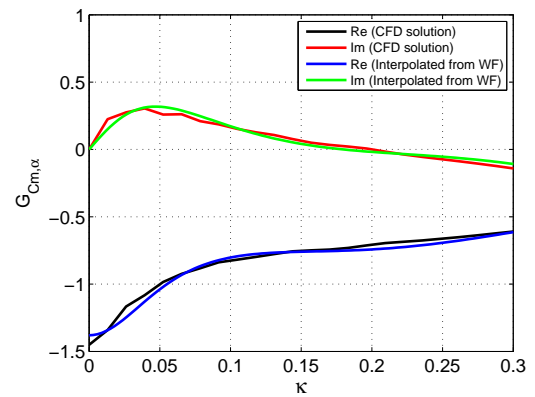
(a) $G_{C_{m,h}}$, normal region of study.



(b) $G_{C_{m,h}}$, detail for very low reduced frequency.



(c) $G_{C_{m,\alpha}}$, normal region of study.



(d) $G_{C_{m,\alpha}}$, detail for very low reduced frequency.

Figure 4. $G_{C_{m,h}}$ and $G_{C_{m,\alpha}}$ transfer functions at low reduced frequencies.

imated transfer functions are the data in which a flutter stability analysis is based on. A similar comparison for the C_m transfer functions is shown in Fig. 4. As one can see in Figs. 3 and 4, in general, there is good agreement between the sets of results from the approximating polynomials and the original CFD data.

5. CONCLUDING REMARKS

The major motivation for the work is the development of the capability of generating unsteady aerodynamic transfer functions in an efficient way, such that CFD results could be readily incorporated into aeroelastic analysis procedures. In other words, the objective is that the aerodynamic information for aeroelastic stability analyses should cost, at most, two CFD runs, *i.e.*, one steady and one unsteady solution. It should be also clear that the major interest of the approaches here discussed lies in the calculation of transonic flutter boundaries, in which the nonlinearities in the representation of the aerodynamic operator are relevant for the accurate prediction of the phenomena of interest. Furthermore, since a linearization with respect to the modal displacements is implicit in the present approach, the calculation procedure is adequate for flutter analyses, but it may not be suitable for limit-cycle oscillation calculations if the structural displacements become larger.

Results are presented for a NACA 0012 airfoil-based typical section model, for freestream conditions $M_\infty = 0.8$ and $\alpha_0 = 0$. From this stationary condition, the system is perturbed in a prescribed pattern in order to obtain unsteady CFD results. The use of a simultaneous excitation signal is employed and it is shown that the system identification routine is capable of splitting the output into the contribution of each individual mode to the corresponding aerodynamic transfer functions. Finally, it is shown that the discrete strings of transfer function values can be conveniently approximated using selected interpolating polynomials. These interpolating polynomials contain, therefore, the aerodynamic states, which can be used for direct aeroelastic stability analyses in the frequency domain. Since the approximating polynomials here

obtained are in good agreement with similar data in the literature, this means that the procedure implemented accomplishes the desired goal of obtaining the aerodynamic operators for aeroelastic analyses with a single unsteady CFD calculation.

6. REFERENCES

- Azevedo, J.H.A., Azevedo, J.L.F. and Silva, R.G.A., 2012. "Efficient calculation of aerodynamic states for aeroelastic analyses in the frequency domain". AIAA Paper No. 2012-1716, 53rd Structures, Structural Dynamics, and Materials and Co-located Conferences, Honolulu, HI.
- Churchill, R.V., 1974. *Complex Variables and Applications*. McGraw-Hill, New York, NY, 3rd edition.
- Eversman, W. and Tewari, A., 1991. "Consistent rational-function approximation for unsteady aerodynamics". *Journal of Aircraft*, Vol. 28, No. 9, pp. 545–552.
- Hadamard, J., 1893. "Résolution d'une question relative aux déterminants". *Bulletin des Sciences Mathématiques*, Vol. 17, pp. 240–246.
- Isermann, R. and Münchhof, M., 2011. *Identification of Dynamical Systems: An Introduction with Applications*. Advanced Textbooks in Control and Signal Processing. Springer. ISBN 9783540788782.
- Jameson, A. and Baker, T.J., 1987. "Improvements to the aircraft Euler method". AIAA Paper No. 87-0452, 25th AIAA Aerospace Sciences Meeting, Reno, NV.
- Jameson, A. and Mavriplis, D., 1986. "Finite volume solution of the two-dimensional Euler equations on a regular triangular mesh". *AIAA Journal*, Vol. 24, No. 4, pp. 611–618.
- Jameson, A., Schmidt, W. and Turkel, E., 1981. "Numerical solution of the Euler equations by finite volume methods using Runge-Kutta time-stepping schemes". AIAA Paper No. 81-1259, 14th AIAA Fluid and Plasma Dynamics Conference, Palo Alto, CA.
- Kim, T., Hong, M., Bhatia, K.G. and SenGupta, G., 2005. "Aeroelastic model reduction for affordable computational fluid dynamics-based flutter analysis". *AIAA Journal*, Vol. 43, No. 12, pp. 2487–2495.
- Kroll, N. and Jain, R.K., 1987. "Solutions of the two-dimensional euler equations – experience with a finite volume code". DFVLR-FB, DFVLR, Braunschweig, Germany.
- Marques, A.N. and Azevedo, J.L.F., 2008a. "Numerical calculation of impulsive and indicial aerodynamic responses using computational aerodynamics techniques". *Journal of Aircraft*, Vol. 45, No. 4, pp. 1112–1135. doi:10.2514/1.32151.
- Marques, A.N. and Azevedo, J.L.F., 2008b. "A z-transform discrete-time state-space formulation for aeroelastic stability analysis". *Journal of Aircraft*, Vol. 45, No. 5, pp. 1564–1578. doi:10.2514/1.32561.
- Mavriplis, D.J., 1990. "Accurate multigrid solution of the Euler equations on unstructured and adaptative meshes". *AIAA Journal*, Vol. 28, No. 2, pp. 545–552.
- McDevitt, J.B. and Okuno, A.F., 1985. "Static and dynamic pressure measurements on a NACA 0012 airfoil in the Ames High Reynolds Number Facility". NASA TP-2485, NASA Ames Research Center, Moffett Field, CA.
- Raveh, D.E., 2001. "Reduced-order models for nonlinear unsteady aerodynamics". *AIAA Journal*, Vol. 39, No. 8, pp. 1414–1429.
- Raveh, D.E., 2004. "Identification of computational-fluid-dynamics based unsteady aerodynamic models for aeroelastic analysis". *AIAA Journal*, Vol. 41, No. 3, pp. 620–632.
- Silva, W.A., 2008. "Simultaneous excitation of multiple-input/multiple-output CFD-based unsteady aerodynamic systems". *Journal of Aircraft*, Vol. 45, No. 4, pp. 1267–1274. doi:10.2514/1.34328.
- Sylvester, J.J., 1867. "Thoughts on inverse orthogonal matrices, simultaneous sign successions, and tessellated pavements in two or more colours, with applications to newton's rule, ornamental tile-work, and the theory of numbers". *Philosophical Magazine Series 4*, Vol. 34, No. 232, pp. 461–475. doi:10.1080/14786446708639914.

7. RESPONSIBILITY NOTICE

The authors are the only responsible for the printed material included in this paper.